Applied Clay Science 99 (2014) 229–236

Contents lists available at ScienceDirect

Applied Clay Science

journal homepage: www.elsevier.com/locate/clay

Research paper

Silylation of Al_{13}-intercalated montmorillonite with trimethylchlorosilane and their adsorption for Orange II

Zonghua Qin [a,b], Peng Yuan [b,*], Shuqin Yang [a], Dong Liu [b], Hongping He [b], Jianxi Zhu [b]

[a] State Key Laboratory of Ore Deposit Geochemistry, Institute of Geochemistry, Chinese Academy of Sciences, Guiyang 550002, China.
[b] CAS Key Laboratory of Mineralogy and Metallogeny, Guangzhou Institute of Geochemistry, Chinese Academy of Sciences, Guangzhou 510640, China

ARTICLE INFO

Article history:
Received 16 September 2013
Received in revised form 6 June 2014
Accepted 17 June 2014
Available online 19 July 2014

Keywords:
Trimethylchlorosilane
Intercalation
Montmorillonite
Grafting
Adsorption
Orange II

ABSTRACT

The grafting reactions between trimethylchlorosilane (TMCS) and Al_{13}-intercalated montmorillonite were investigated using X-ray diffraction, Fourier transform infrared spectroscopy, thermogravimetric analysis, and nitrogen adsorption–desorption isotherms. The influence of solvent on the grafting process is discussed. The grafting amount of TMCS was roughly controlled by choosing different solvents. The product prepared in anhydrous ethanol has a high specific surface area and a large pore volume but a low degree of grafting modification; by comparison, the product prepared in cyclohexane has a high loading amount of silane but a low surface area. These organic–inorganic montmorillonites have an excellent adsorption capability for the removal of the anion dye, Orange II. Orange II exists in the interlayer region, not only through the electrostatic interactions between the anionic sulfonic acid groups of Orange II and the interlayer Al polycations, but also through the hydrophobic interactions between Orange II molecules and grafted silane. With particular emphasis on the absorbents prepared in cyclohexane, the removal rate of Orange II remains at 98.7% when the initial concentration is 1000 mg l^{-1}. A continuous organic phase is formed in the interlayer space of the products prepared in cyclohexane. The removal of Orange II with this adsorbent is based on both the adsorption on the interface and the partition between the water and the interlayer organic phases.

1. Introduction

Montmorillonite is widely used as an adsorbent for pollutant removal, because it is widespread, inexpensive and environmentally friendly (Bergaya et al., 2006b). However, the removal of anionic organic pollutants that are abundant in the environment by montmorillonite is difficult due to the negatively charged surface and hydrophilicity of montmorillonite. Generally, inorganic pillaring or organic intercalation is used to enhance the adsorptive capacity of montmorillonite.

With respect to inorganic pillaring, polyoxometal cations in which the central element is composed of Al (Kloprogge, 1998; Moreno et al., 1997; Salerno and Mendioroz, 2002; Sivaiah et al., 2010), Fe (Valverde et al., 2005; Yuan et al., 2006a, 2008a), or Ti (Vicente et al., 2001; Valverde et al., 2003; Yuan et al., 2006b), and two or more metal elements (Bergaya et al., 2006a) enter the interlayer space of montmorillonite by cation exchange, and then are transformed into metal oxide pillars by calcination. After modification, the resulting pillared montmorillonite has a larger specific surface area, better porous structure and higher surface acidity. All of these properties are favorable for adsorption, especially for the adsorption of anionic pollutants with small molecular volume, such as phosphate (Kasama et al., 2004), arsenate (Na et al., 2010; Peng et al., 2005), nitrate, sulfate, and chloride (Aouad et al., 2006) that are not readily removed by the unmodified montmorillonite precursor. However, modification with inorganic species does not change the hydrophilicity of montmorillonite, and the transformation from polyoxometal cations to oxides decreases the positive charges in the interlayer space, thus the removal capacity of pillared montmorillonite for anionic organic pollutants with large molecular volume does not meet expectations.

The organic intercalation of montmorillonite can significantly enhance the organophilicity of the resultant product. Cationic organic compounds, such as surfactant cations, exchange the interlayer cations of montmorillonite (de Paiva et al., 2008; He et al., 2006; Lagaly, 1986; Xi et al., 2007), and the resulting organoclay is excellent for diverse organic pollutants, e.g. phenol (Banat et al., 2000; Juang et al., 2002; Zhou et al., 2008), dye (Baskaralingam et al., 2006; Ozcan et al., 2007), and VOCs (Jarraya et al., 2010; Park et al., 2008; Tian et al., 2004). Nevertheless, surfactant molecules which are easily extracted from the interlayer space towards the solution with the fluctuation of the ambient environment, such as pH, can become new pollutants, because the link between the cationic surfactant molecules and the

* Corresponding author at: Guangzhou Institute of Geochemistry, Chinese Academy of Sciences, Wushan, Guangzhou 510640, China. Tel.: +86 20 85290341; fax: +86 20 85290130.
E-mail address: yuanpeng@gig.ac.cn (P. Yuan).

http://dx.doi.org/10.1016/j.clay.2014.06.038
0169-1317/

montmorillonite layer is weak. Moreover, many surfactant molecules inhabit the interlayer space, resulting in a prominent decrease in the specific surface area of organo-montmorillonite.

To overcoming these drawbacks, numerous attempts have been made to combine the advantages of inorganic and organic modification. For example, Jiang and coworkers utilized hexadecyltrimethylammonium bromide to modify Al/Fe-pillared montmorillonite and investigated its adsorption capacity for phenol (Jiang et al., 2002). Zhu's group prepared an intercalated montmorillonite with both hexadecyltrimethylammonium bromide and Al_{13} cations, and discussed the influence of the addition sequence of these two modifiers on the final products (Zhu and Zhu, 2007). However, the shortcomings of the organo-montmorillonite (such as low specific surface area and pore volume) still remain.

Compared to intercalation with surfactants, modification using organosilane is based on the condensation reaction between the silanols resulting from the hydrolysis of organosilane and the Si–;OH and/or Al–OH of clay minerals. The grafting of clay minerals with organosilanes would achieve chemically covalent bindings between organic compounds and clay minerals, and it is more stable than the electrostatic interactions between surfactants and clay minerals. Voluminous papers have focused on the organosilane grafting of clay minerals (Bourlinos et al., 2004; Breiner et al., 2006; Guimaraes et al., 2009; He et al., 2005; Shanmugharaj et al., 2006; Shen et al., 2007; Yuan et al., 2008b), but little work has been conducted for the grafting of intercalated clay minerals, such as Al_{13}-intercalated montmorillonite.

The hydrolysis of organosilanes and the condensation of the hydrolysates or the surface hydroxyls of clay minerals are the key factors affecting the structures and properties of the final products. In particular, for the grafting of Al_{13}-intercalated montmorillonite, the solvent that was used for the reaction is significant to the process of grafting.

Based on the above consideration, in this study trimethylchlorosilane (TMCS), which has hydrophobic methyl groups, was used to modify Al_{13}-intercalated montmorillonite. TMCS is a silane which has only one hydrolyzed group (–Cl) for silylation of Al_{13}-intercalated montmorillonite and three methyl groups that can effectively control the amount of grafting. The structures and formation mechanisms for the grafted products in two solvents with different polarity, anhydrous ethanol and cyclohexane, were discussed. Finally, Orange II, an anionic organic dye, was selected as a target pollutant for evaluating the adsorptive capacity of the silane-modified products, and the mechanism for these adsorption processes was investigated. We anticipate that this research will promote the understanding of organic–inorganic modified montmorillonite, and broaden its application in the disposal of environmental pollutants.

2. Experimental section

2.1. Materials

The montmorillonite (Mt) used in this study was from Inner Mongolia, China. The cation exchange capacity (CEC) was 1.06 meq/g. The chemical composition (wt.%) of Mt determined from chemical analysis is as follows: SiO_2, 49.44; Al_2O_3, 15.94; Fe_2O_3, 2.47; CaO, 4.36; MgO, 4.02; K_2O, 0.13; Na_2O, 0.52; MnO, 0.015; TiO_2, 0.31; and L.O.I., 22.55. It was used without further purification. Trimethylchlorosilane (TMCS) with a purity of 99.0% was supplied by Sigma-Aldrich, Inc. All the chemicals and reagents used in this work were of analytical grade and used as received.

2.2. Synthesis of Al_{13}-intercalated montmorillonite and its thermally treated derivatives

Al_{13}-intercalated montmorillonite was prepared as that in a previous study (Qin et al., 2010). This intercalated sample was denoted as Al_{13}-Mt.

2.3. Methods of organosilane modification

The Al_{13}-Mt (10 g) was added to 200 ml anhydrous ethanol in a flask. This mixture was treated by ultrasound at 60 °C for 10 min. Then, 5 ml TMCS was added to the mixture with fast stirring. The dispersion was refluxed at 80 °C for 20 h at a stirring rate of 400 rpm. The products were washed 6 times with anhydrous ethanol by centrifugation. The solids were oven dried at 80 °C, ground and sealed in polyethylene bottles. Based on the raw materials and the solvent, the final powder was denoted as Al_{13}-Mt/E.

Following the same procedures mentioned above and using cyclohexane as the solvent to replace anhydrous ethanol, the organosilane-modified sample was prepared, denoted as Al_{13}-Mt/C.

2.4. Adsorption tests

For the adsorption tests, 0.1 g unmodified/modified montmorillonite and 25 ml Orange II solution with a concentration of 100, 200, 300, 400, 500, 600, 700, 800, 900, or 1000 mg l^{-1} were added to ten conical flasks (50 ml) with a stopper. The pH values of these dispersions were adjusted to 6.8 using HCl and NaOH solutions. The flasks were placed into a shaker at 20 °C for 12 h at a speed of 150 rpm. The dispersions were centrifuged at 3500 rpm, and the supernatants were analyzed in an ultraviolet–visible spectrophotometer at a wavelength of 484 nm (the maximum absorption wavelength of Orange II). The equilibrium concentration (C_e) was calculated according to the standard curve and the equilibrium adsorption amount (q_e) as derived by:

$$q_e = (C_0 - C_e)V/W \tag{1}$$

where q_e is the equilibrium adsorption amount (mg g^{-1}), C_0 is the initial concentration of Orange II (mg l^{-1}), C_e is the equilibrium concentration of Orange II (mg l^{-1}), V is the volume of the solution (ml), and W is the mass of the adsorbent (g).

The Langmuir model (Ho and McKay, 1998), Freundlich model (Vadivelan and Kumar, 2005), Temkin model (Kim et al., 2004) and Redlich–Peterson model (Wang et al., 2005) are all used for fitting the adsorption isotherms and interpreting the adsorption mechanism:

The Langmuir model is shown as:

$$q_e = \frac{q_m K_L C_e}{1 + K_L C_e} \quad \frac{C_e}{q_e} = \frac{1}{K_L q_m} + \frac{1}{q_m} C_e \tag{2}$$

where q_m and K_L are the Langmuir constants, representing the maximum adsorption capacity for solid phase loading, and the energy constant, which is related to the heat of adsorption, respectively.

The Freundlich model is:

$$q_e = K_F C_e^{\frac{1}{n_F}} \quad \log q_e = \log K_F + \frac{1}{n_F} \log C_e \tag{3}$$

where K_F is the Freundlich equilibrium constant indicating the relative adsorption capacity of the adsorbent, and $1 / n_F$ is an arbitrary constant evaluated by linearizing the equation.

The Temkin model is:

$$q_e = B_T \ln(K_T C_e) \quad q_e = B_T \ln K_T + B_T \ln C_e \tag{4}$$

where K_T is a constant of the Temkin isotherm, and B_T is a Temkin isotherm constant related to the heat of adsorption.

The Redlich–Peterson model is written as:

$$q_e = \frac{A_R C_e}{1 + B_R C_e^{\beta_R}} \tag{5}$$

where A_R and B_R are the constants of Redlich–Peterson isotherm, and β_R is the empirical constant with values that range $0 < \beta_R < 1$.

2.5. Characterization methods

The basal spacings of these powders were determined by X-ray diffraction (XRD) using a Bruker D8 Advanced Diffractometer equipped with Ni-filtered Cu Kα radiation (λ = 0.154 nm) and operating at 40 kV and 40 mA with a fixed slit. The scan rate was 1.0° (2θ) min^{-1} and the scanning range was from 1° to 30° (2θ).

FTIR spectra were obtained using a Bruker VERTEX 70 Fourier transform infrared spectrometer. The KBr pellets were prepared by pressing mixtures of 0.9 mg powder with 80 mg KBr. All the spectra were collected at room temperature over 4000–400 cm^{-1} with a resolution of 4 cm^{-1} and 64 scans.

TG–DTG curves were obtained using a NETZSCH STA 409 thermal analyzer. The samples were heated with the rate of 10 °C min^{-1} under a flow of high purity nitrogen from 30 to 1000 °C.

Nitrogen adsorption–desorption isotherms were measured on a Micromeritics ASAP 2020M instrument. Before the adsorption tests, the samples were outgassed under a vacuum for 12 h at 100 °C. The multiple-point Brunauer–Emmett–Teller (BET) method was used to calculate the specific surface areas of the samples.

3. Results and discussion

3.1. X-ray diffraction

The XRD pattern of montmorillonite (Fig. 1a) has a characteristic (001) reflection at approximately 5.86° (2θ) with a spacing of 1.51 nm that is attributed to Ca-montmorillonite. The basal spacing (d_{001}) of Al_{13}-Mt is 1.89 nm (Fig. 1b). It corresponds to the interlayer space of Al_{13}-Mt (0.93 nm), thus providing important argument for the successful intercalation of hydroxyaluminum polycation (Al_{13}^{7+}) with size of approximately 0.9 nm. The sharp (001) reflection indicates a high degree of order.

After modification by TMCS, the XRD pattern of the sample prepared in anhydrous ethanol (Fig. 1c) shows few change except for a slight decrease in the (001) intensities. However, for the sample prepared in cyclohexane (Fig. 1d), the (001) reflection significantly broadens and its intensity decreases. It shows that there are some amorphous phases that result from the grafted organosilanes in the interlayer space of the intercalated montmorillonite for the modified sample and these substances decrease the overall degrees of ordering of the samples. Comparing the (001) intensities of these two samples, we speculate that more silane molecules enter the interlayer space of Al_{13}-Mt/C than Al_{13}-Mt/E.

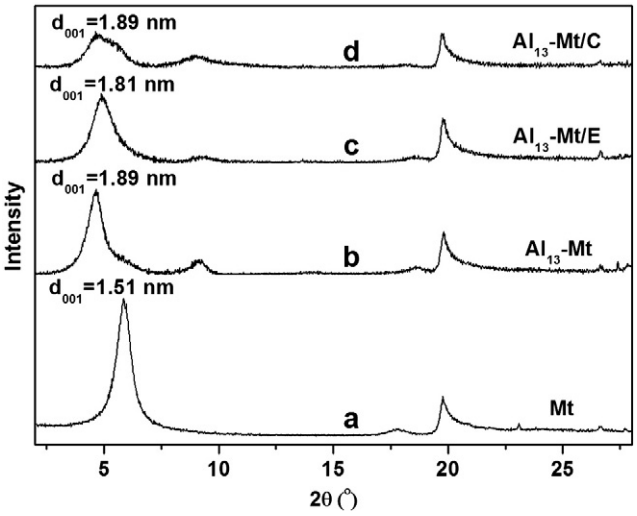

Fig. 1. XRD patterns of the samples before and after TMCS modification.

3.2. FTIR spectra

The FTIR spectra of the samples are shown in Fig. 2, and their assignments are listed in Table 1. For Mt (Fig. 2a) and Al_{13}-Mt (Fig. 2b), the band at 3614 cm^{-1} is assigned to the stretching vibration of octahedral OH groups which are attached to Al^{3+} or Mg^{2+} (Bukka et al., 1992). The peak intensity of Al_{13}-Mt is significantly stronger than that of Mt, due to the contribution of hydroxyl groups on the interlayer Al_{13} cations of Al_{13}-Mt. The absorption bands in the 700–1500 cm^{-1} region are primarily assigned to stretching vibrations of the Si – O(– Si) bonds and the deformation modes of OH groups attached to various ions (e.g., $A1^{3+}$, Mg^{2+} and Fe^{3+}). The band observed at 916 cm^{-1} is assigned to OH groups attached to $A1^{3+}$ ions.

The new adsorption peaks of the silylated samples at 2962 and 2931 cm^{-1} (the inset of Fig. 2a) are attributed to the asymmetric stretching of C – H and the band at 2854 cm^{-1} is caused by the symmetric stretching of C – H. The C – H signals of the silylated samples prepared in cyclohexane are more significant than the samples prepared in anhydrous ethanol. This shows that the grafting reaction can proceed more easily in cyclohexane than in anhydrous ethanol. Meanwhile, the bands at 1036 cm^{-1} of the silylated samples become wider comparing with Mt and Al_{13}-Mt, and this phenomenon of Al_{13}-Mt/C is more obvious than that of Al_{13}-Mt/E. It also suggests that the samples prepared in cyclohexane have high loading amounts of TMCS.

3.3. Thermal analysis

The TG and DTG curves of the samples before and after grafting are shown in Fig. 3. The DTG curves of Mt (Fig. 3a) display two peaks at 117 and 167 °C, corresponding to loss of the physically adsorbed water on the external surface and within the interlayer spaces of Mt. Additionally, the peak at 724 °C is attributed to the dehydroxylation of octahedral sheet.

Two significant mass losses in the curves for Al_{13}-Mt can be identified (Fig. 3b). The first one occurs between 30 and 300 °C, while the DTG curve peak at ~100 °C. The corresponding mass loss is 14.23 wt.%. It seems to be consistent with that of Na-montmorillonite at this temperature. These mass losses are due to the removal of physisorbed water on the surface and within the interlayer space of the intercalated montmorillonite. The second mass loss occurs between 300 and 700 °C, suggested by the DTG curve peaks at 503 °C. The mass loss is 8.92%, which is attributed to the dehydroxylation of interlayer Al_{13} compounds and the octahedral sheets of montmorillonite. For Al_{13}-Mt, the dehydroxylation of the interlayer Al compounds that appear between 350 °C and 500 °C overlaps with the dehydroxylation of the montmorillonite layers, resulting in the mass loss at ~500 °C.

For the Al_{13}-Mt/E (Fig. 3c), the TG–DTG curve has little change comparing with the intercalated sample (Al_{13}-Mt). The peaks at 103 °C and 509 °C in the DTG curve are attributed to the removal of physically adsorbed water and hydroxyl of Al_{13}-pillared montmorillonite, respectively. Because of the small amounts of grafting within the samples prepared in anhydrous ethanol, the decomposition of the few grafting silanes results in mass loss peak at 345.2 °C.

The DTG curve of Al_{13}-Mt/C (Fig. 3d) is similar to that of Al_{13}-Mt/E. However, the first mass loss peak shifts to high temperature (169 °C) and there is a larger mass loss between 300 and 500 °C. This result illustrates that the samples modified in cyclohexane have more grafted silane than those modified in anhydrous ethanol. Large amounts of silanes enter the interlayer spaces of Al_{13}-intercalated montmorillonite, resulting in the crosslinking of some silanes by oligomerization or exist in the form of monomer molecules adsorbed on the montmorillonite matrix, rather than react with the Al_{13} cations. These silanes will escape at a lower temperature than those which react with interlayer cations,

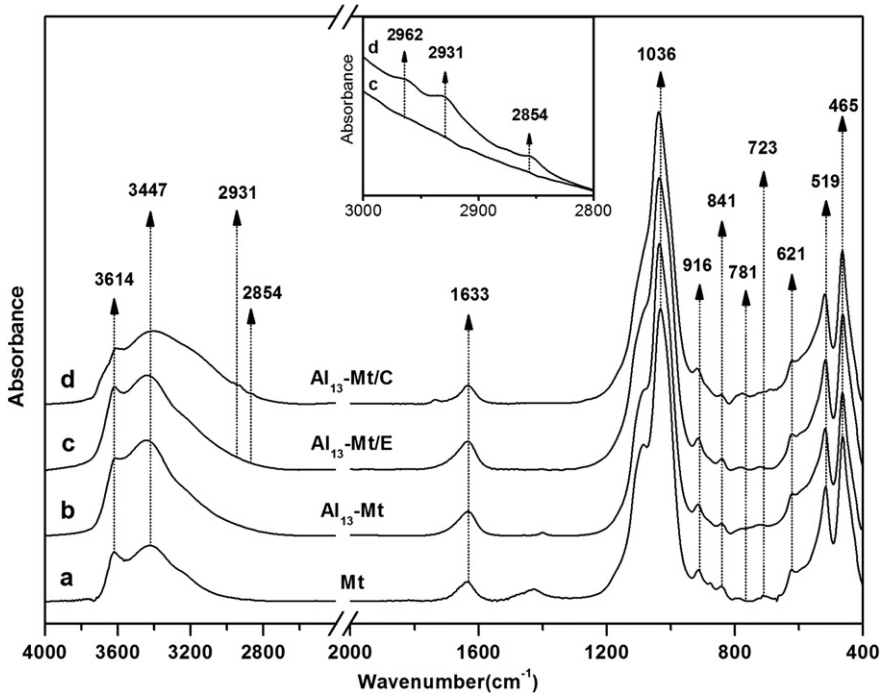

Fig. 2. FTIR spectra of the samples before and after TMCS modification.

and the volatilization of these silanes forms the peak at 169 °C together with removal of physically adsorbed water.

3.4. Nitrogen adsorption–desorption isotherms

The nitrogen adsorption and desorption isotherms of the samples are shown in Fig. 4. According to IUPAC-classification (Gregg and Sing, 1967), the adsorption isotherms of the samples all belong to type IV, suggesting that the samples had mesoporous structure. The shape of hysteresis loops from 0.4 to 0.9 of relative pressure was of a type H3, inducing by the slit-shaped pores whose sizes were not well-proportioned (Sing et al., 1985).

The N_2 adsorbed amount of Mt is very small at low relative pressure, but increases steeply at high pressure, which is caused by the adsorption on the macropores fabricated by "card-house" structure. The hysteresis loop of Mt has a large area, and obvious hysteresis at $p/p_0 = 0.4–1.0$ suggests that capillary condensation is taking place in pores.

The nitrogen quantity adsorbed onto Al_{13}-Mt is obviously higher than that of raw montmorillonite, and this shows that the intercalation of Al_{13} can significantly develop the porous structure of montmorillonite. The small area of loop and little hysteresis are indicating that the shape of pores in the sample is close to cylinder, and the pore size is uniform.

After TMCS modification (Fig. 4b), the quantity of adsorbed nitrogen is reduced sharply, especially for the samples prepared in cyclohexane. The samples prepared in anhydrous ethanol have higher nitrogen quantity adsorbed than those prepared in anhydrous ethanol, and this is indicative of an abundant porous structure. Comparing with those of the unmodified samples, the hysteresis loops of the N_2 adsorption–desorption isotherms of the silane-modified samples show very similar shapes (type H3) but are less developed. These findings suggest that the mesoporosity of the modified samples is decreased.

The specific surface areas and total pore volumes of the modified and unmodified samples are presented in Fig. 5. The specific surface area of Al_{13}-Mt is four times greater than that of Mt, but the difference of the total pore volumes is small, thereby demonstrating that the micropores are in the majority after the intercalation of Al_{13}. The samples prepared in anhydrous ethanol have higher specific surface areas and total pore volumes compared to those prepared in cyclohexane. The specific surface area and total pore volume of Al_{13}-Mt/E are 176 $m^2\ g^{-1}$ and 0.194 $cm^3\ g^{-1}$, respectively. These data also demonstrate the porous structure associated with this sample. However, for Al_{13}-Mt/C, the specific surface area and total pore volume are only 21 $m^2\ g^{-1}$ and 0.053 $cm^3\ g^{-1}$, respectively. This result demonstrates the large grafting amounts in these samples and that the pore structure is blocked by silane molecules. These results are also in agreement with the results of the FTIR spectra and the TG–DTG analysis.

Table 1
Positions and assignments of the FTIR vibration bands.

Position (cm^{-1})	Assignments
3614	– OH stretching of Al – OH and Mg – OH
3447	– OH stretching of interlayer water
2962	Asymmetric stretching of C – H
2931	Asymmetric stretching of C – H
2854	Symmetric stretching of C – H
1633	– OH deformation of interlayer water
1036	Si – O stretching
916	– OH deformation of Al^{VI} – OH
841	– OH deformation of Mg^{VI} – OH
781	Si – O Stretching of quartz
723	Stretching of Si – O
621	Stretching of Si – O – Si(Al)
519	Deformation of Si – O – Al^{VI}
465	Deformation of Si – O – Si

3.5. Modification mechanism of Al_{13}-intercalated montmorillonite with TMCS

The reactions that occur in anhydrous ethanol are different from those that occur in cyclohexane. Ethanol can react with chlorosilane, thereby forming trimethylethoxysilane whose hydrolysates contain ethanol. Therefore, the silylation process is restrained in the anhydrous ethanol system. Moreover, ethanol is a polar solvent. The interactions of

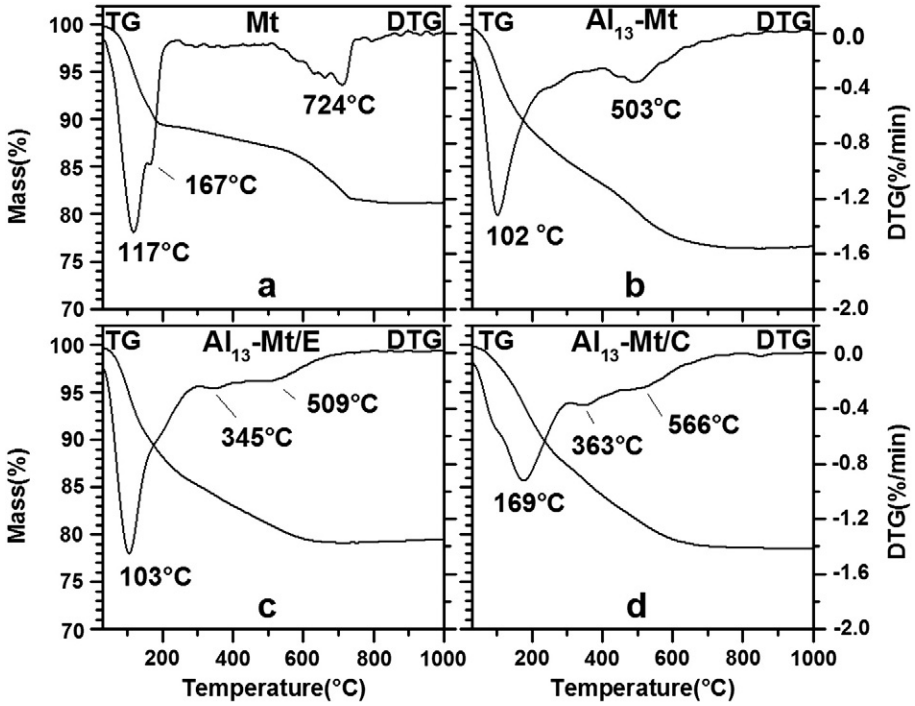

Fig. 3. TG and DTG curves of the samples before and after TMCS modification.

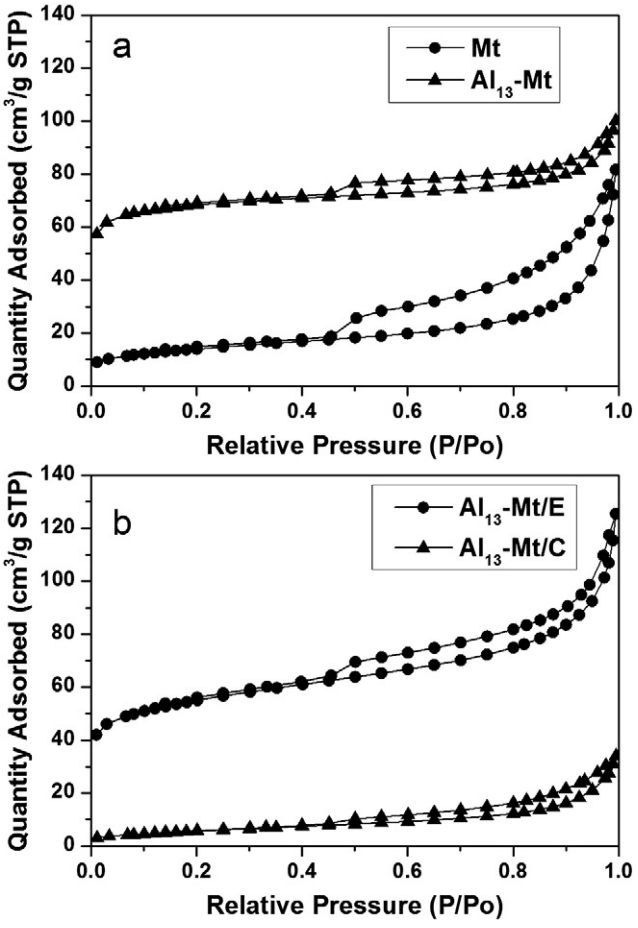

Fig. 4. Nitrogen adsorption–desorption isotherms of the samples before and after TMCS modification.

siloxane with ethanol are stronger than those with apolar cyclohexane, and thus, fewer TMCS molecules are diffused into the interlayer space of Al_{13}-intercalated montmorillonite, leading to comparatively little grafting. However, in the cyclohexane system, there are few interactions between TMCS and cyclohexane; thus, more TMCS molecules may react with the Al_{13}-intercalated montmorillonite or condensate with each other forming oligomers, contributing to the high loading amounts of silane. The reactions that occur in the two solvent systems are listed as follows.

In anhydrous ethanol:

$$(CH_3)_3Si\text{–}Cl \xrightarrow{CH_3CH_2OH} (CH_3)_3SiOCH_2CH_3 + HCl$$

$$(CH_3)_3SiOCH_2CH_3 + H_2O \rightarrow (CH_3)_3SiOH + CH_3CH_2OH$$

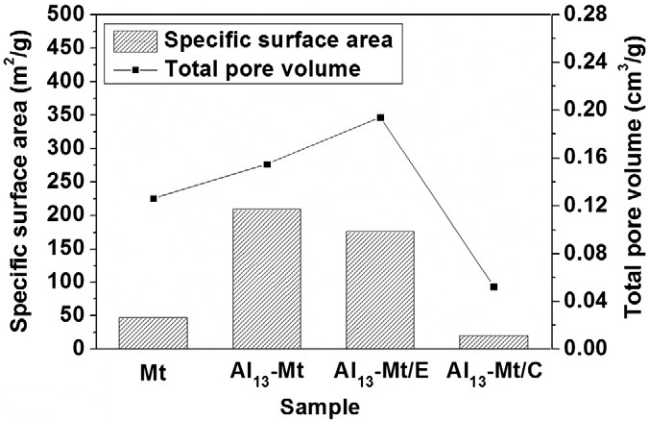

Fig. 5. BET specific surface areas and total pore volumes of the TMCS-modified sample.

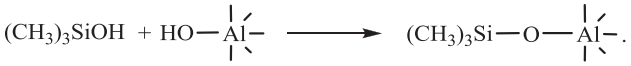

In cyclohexane:

$$(H_3C)_3Si\text{–}Cl + H_2O \rightarrow (CH_3)_3SiOH + HCl$$

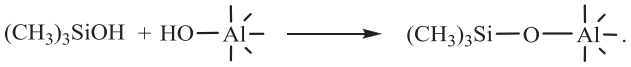

$$2(CH_3)_3SiOH \rightarrow (CH_3)_3SiO(CH_3)_3.$$

In these reactions,  is the hydroxyl group on the interlayer Al_{13} cations of the Al_{13}-intercalated montmorillonite.

3.6. Adsorption isotherm analysis

The fitting results of montmorillonite (Mt), Al_{13}-intercalated montmorillonite (Al_{13}-Mt), and the modified samples prepared in anhydrous ethanol (Al_{13}-Mt/E) and cyclohexane (Al_{13}-Mt/C) are shown in Table 2.

The adsorption isotherm for Orange II on montmorillonite is consistent with the Redlich–Peterson model. Because of $\beta_R \ll 1$, the adsorption pattern is significantly different from the Langmuir isotherm model (i.e., non-monolayer adsorption). The adsorption isotherm also fits the Freundlich model, when R^2 is close to 1. The extremely small K_F value suggests that there is little adsorption capacity of montmorillonite for Orange II, and the small n_F value illustrates the weak interaction between the montmorillonite and the Orange II molecules.

The adsorption isotherm of Al_{13}-intercalated montmorillonite (Al_{13}-Mt) is of a Langmuir isotherm type. The saturated adsorption amount (Q_m) is 100 mg g^{-1}. The arrangement of Orange II molecules on Al_{13}-Mt adopts a monolayer.

The adsorption isotherm of the modified sample prepared in anhydrous ethanol (Al_{13}-Mt/E) is fit to a Langmuir model. Its saturated adsorption amount (Q_m) is 118.6 mg g^{-1}, which is higher than that of Al_{13}-Mt. The larger K_L of Al_{13}-Mt/E illustrates that the interactions of Orange II molecules with Al_{13}-Mt/E are stronger than those with Al_{13}-Mt.

Adsorption of the modified sample prepared in cyclohexane (Al_{13}-Mt/C) is attributed to the Temkin adsorption model. The Temkin adsorption isotherm model is based on the assumption that the distribution of the surface binding energies is uniform, thus, there is a random distribution of surface binding sites. A large B_T value suggests a high adsorption amount for Orange II. The random distribution of functional groups for adsorption and the high density of the adsorbate consequentially result in the complex interaction between Orange II molecules and the adsorbent. Hence, the surface morphology of this adsorbent and the existential state of the adsorbate are more complicated than the aforementioned samples.

The adsorption energy can be calculated using the K_T value according to the Arrhenius equation: $K = e^{-\frac{\Delta G}{RT}}$, where K is the rate coefficient, ΔG is the Gibbs free energy, R is the universal gas constant (8.314×10^{-3} kJ mol^{-1} K^{-1}), and T is the temperature (in Kelvin) (Kim et al., 2004).

$$\Delta G = -RT \ln K = -8.31 \times 293.15 \times \ln\left(0.621 \times 350.330 \times 10^3\right) = -29.9 \text{ kJ mol}^{-1}$$

The high B_T value suggests that there are a large number of Orange II molecules adsorbed at each binding energy, and these are suggestive of weak interactions between the adsorbent and Orange II.

The adsorption isotherms of the samples are given in Fig. 6. The adsorption amount of Orange II onto montmorillonite is small. Al_{13} intercalation can substantially increase the adsorption capacity. Moreover, organic modifications can further enhance the adsorption behavior. The saturated adsorption amount on Al_{13}-Mt/E is 120 mg l^{-1}, and this is higher than the value for Al_{13}-Mt (100 mg l^{-1}). The modified sample in the cyclohexane system (Al_{13}-Mt/C) has the best adsorption capacity among these adsorbents. Its adsorption isotherm approximates a perpendicular line in the concentration range that we attempted, and this implies that it is far from saturated adsorption. The adsorption amount of this sample is close to 250 mg g^{-1}, and obviously higher than that of the other samples.

From the removal efficiency curves (Fig. 7), the adsorption capacities of these samples are more easily determined: Al_{13}-Mt/C > Al_{13}-Mt/E > Al_{13}-Mt > Mt. With respect to Al_{13}-Mt/C, the removal efficiency remains at 98.7% even when the initial concentration of Orange II is 1000 mg l^{-1}.

3.7. Adsorption mechanism

The hypothetical adsorption patterns of Orange II on these montmorillonite-based materials are shown in Fig. 8.

The layers of montmorillonite are negatively charged, and there is electrostatic repulsion between the layers and the anions. Hence, anions are difficult to adsorb on the surface of montmorillonite. Little adsorption for Orange II occurs from the "broken bonds" on the edge of the layers that bind the ambient cations.

Table 2
Fitting parameters of the adsorption isotherm of Mt, Al_{13}-Mt, Al_{13}-Mt/E, and Al_{13}-Mt/C.

Adsorption models	Parameters	Mt	Al_{13}-Mt	Al_{13}-Mt/E	Al_{13}-Mt/C
Langmuir	q_m	–	100.100	118.624	–
	K_L	–	0.093	0.115	–
	R^2	–	0.998	0.999	–
Freundlich	n_F	0.509	4.390	3.752	0.904
	K_F	1.100×10^{-5}	26.596	27.174	18.229
	R^2	0.993	0.859	0.812	0.855
Temkin	B_T	2.939	13.26	17.679	116.904
	K_T	0.006	4.634	2.721	0.621
	R^2	0.792	0.949	0.915	0.994
Redlich–Peterson	A_R	0.009	20.447	11.720	21.562
	B_R	87,801.821	0.336	0.102	−52.90
	β_R	−1.873	0.91844	0.991	−65.770
	R^2	0.997	0.961	0.977	0.900

– represents fitting results that are not convergent or the R^2 is negative.

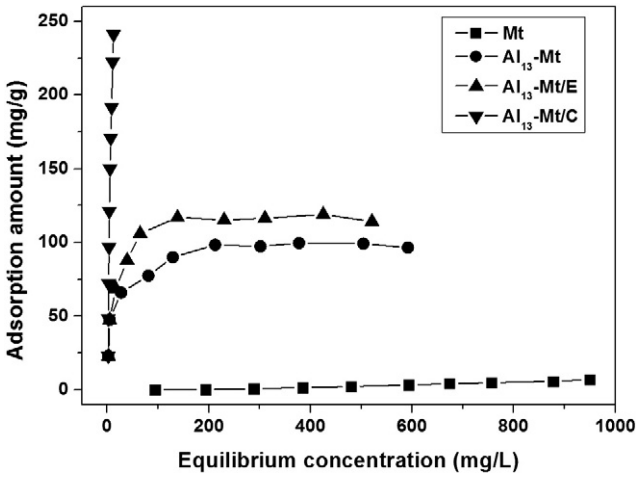

Fig. 6. Adsorption isotherms of Mt, Al_{13}-Mt, Al_{13}-Mt/E and Al_{13}-Mt/C.

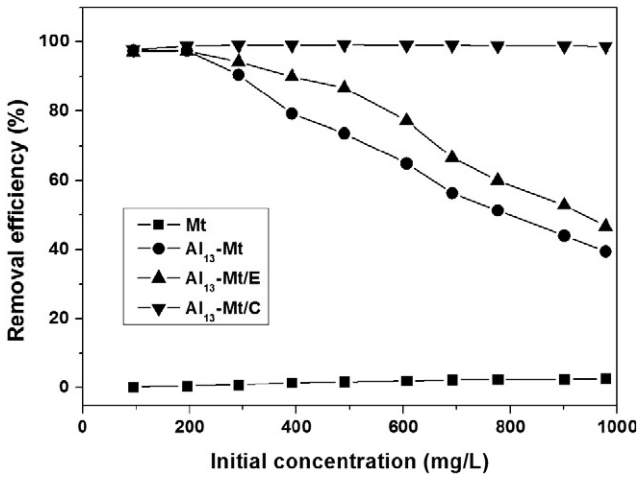

Fig. 7. Removal rates of Orange II for Mt, Al_{13}-Mt, Al_{13}-Mt/E and Al_{13}-Mt/C.

Al_{13}-intercalated montmorillonite possesses a higher specific surface area than raw montmorillonite; the interlayer distance increases after Al_{13} intercalation, and electrostatic repulsion hindering the diffusion of anions into the interlayer spaces becomes weak. These both favor adsorption. Meanwhile, Al Keggin ions ($[Al_{13}O_4(OH)_{24}(H_2O)_{12}]^{7+}$) have high-valent centralized positive charges that favor anion binding and adsorption. The adsorption of Orange II on Al_{13}-intercalated montmorillonite is based on electrostatic interactions between the Al Keggin cations and the negatively charged sulfonic groups of the Orange II molecules. Due to the overall hydrophilicity of Al_{13}-Mt and the large molecular volume of the Orange II molecule (409 $Å^3$, obtained by theoretical calculation), steric hindrance limits the further adsorption on Al_{13}-Mt.

After silane modification, the surface of montmorillonite changes from hydrophilic to hydrophobic and its binding capacity with organic molecules is enhanced. The adsorption process of these silylated samples is based on not only the electrostatic attraction between the sulfonic groups and the interlayer Al Keggin cations, but also the intermolecular forces (that are weaker than electrostatic interaction) between the aromatic rings of the Orange II molecules and the grafted silanes. For the sample modified in anhydrous ethanol (Al_{13}-Mt/E), which has lower loading amounts of TMCS, the increase of its adsorption capacity is finite. However, for Al_{13}-Mt/C with high loading amounts of silanes, a continuous organic phase is formed in the interlayer spaces of montmorillonite. Here, a partition of Orange II between the solvent and the interlayer organic phase also contributes to the removal of Orange II, in addition to adsorption on the surface. The removal efficiency of Al_{13}-Mt/C is considerably enhanced.

4. Conclusion

Al_{13}-intercalated montmorillonite has been modified by trimethylchlorosilane (TMCS), thereby leading to new absorbents for the removal of aquatic anion pollutants. Solvents for modification can influence the loading amounts of silanes. The samples prepared in anhydrous ethanol maintain a large specific surface area and a fine pore structure, but the samples prepared in cyclohexane have higher loading amounts of TMCS. The reactions that occur in anhydrous ethanol and cyclohexane are different.

Comparing the adsorption isotherms and removal efficiencies of montmorillonite, the Al_{13}-intercalated montmorillonite and the silylated samples in anhydrous ethanol and cyclohexane system, our data suggest that the removal capacity of the modified sample prepared in cyclohexane is the best. For the silylated samples, the removal of Orange II is based on not only the electrostatic attraction between the sulfonic groups and the interlayer Al Keggin cations, but also the intermolecular force between the aromatic rings of the Orange II molecules and the grafted silanes. With special regard to the modified sample prepared in cyclohexane (which has a continuous organic phase in the interlayer space), a partitioning of Orange II between the solvent and the interlayer organic phase is as important as adsorption for the removal of Orange II.

Acknowledgments

Financial support from the Team Project of Natural Science Foundation of Guangdong Province, China (Grant No. S2013030014241), National Natural Science Funds for Young Scholar (Grant No. 41202031), and National Key Technology Research and Development Program of

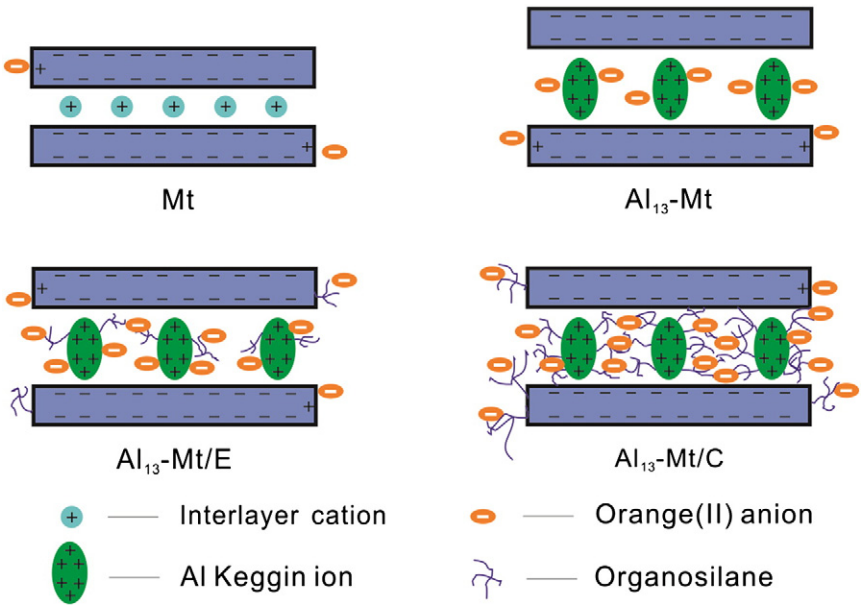

Fig. 8. Adsorption mechanisms of Orange II for Mt, Al_{13}-Mt, Al_{13}-Mt/E and Al_{13}-Mt/C.

the Ministry of Science and Technology of China (Grant No. 2013BAC01B02).

References

Aouad, A., Pineau, A., Tchoubar, D., Bergaya, F., 2006. Al-pillared montmorillonite obtained in concentrated media. Effect of the anions (nitrate, sulfate and chloride) associated with the Al species. Clay Clay Miner. 54 (5), 626–637.

Banat, F.A., Al-Bashir, B., Al-Asheh, S., Hayajneh, O., 2000. Adsorption of phenol by bentonite. Environ. Pollut. 107 (3), 391–398.

Baskaralingam, P., Pulikesi, M., Elango, D., Ramamurthi, V., Sivanesan, S., 2006. Adsorption of acid dye onto organobentonite. J. Hazard. Mater. 128 (2–3), 138–144.

Bergaya, F., Aouad, A., Mandalia, T., 2006a. Pillared clays and clay minerals. In: Bergaya, F., Theng, B.K.G., Lagaly, G. (Eds.), Handbook of Clay Science. Elsevier Science, Amsterdam.

Bergaya, F., Theng, B.K.G., Lagaly, G., 2006b. Clays, environment and health. In: Bergaya, F., Theng, B.K.G., Lagaly, G. (Eds.), Handbook of Clay Science. Elsevier Science, Amsterdam.

Bourlinos, A.B., Jiang, D.D., Giannelis, E.P., 2004. Clay–organosiloxane hybrids: a route to cross-linked clay particles and clay monoliths. Chem. Mater. 16 (12), 2404–2410.

Breiner, J.M., Anderson, M.A., Tom, H.W.K., Graham, R.C., 2006. Properties of surface-modified colloidal particles. Clay Clay Miner. 54 (1), 12–24.

Bukka, K., Miller, J.D., Shabtai, J., 1992. FTIR study of deuterated montmorillonites: structural features relevant to pillared clay stability. Clay Clay Miner. 40 (1), 92–102.

de Paiva, L.B., Morales, A.R., Diaz, F.R.V., 2008. Organoclays: properties, preparation and applications. Appl. Clay Sci. 42 (1–2), 8–24.

Gregg, S.J., Sing, K.S.W., 1967. Adsorption, Surface Area, and Porosity. Academic Press.

Guimaraes, A.D.F., Ciminelli, V.S.T., Vasconcelos, W.L., 2009. Smectite organofunctionalized with thiol groups for adsorption of heavy metal ions. Appl. Clay Sci. 42 (3–4), 410–414.

He, H.P., Duchet, J., Galy, J., Gerard, J.F., 2005. Grafting of swelling clay materials with 3-aminopropyltriethoxysilane. J. Colloid Interface Sci. 288 (1), 171–176.

He, H.P., Frost, R.L., Bostrom, T., Yuan, P., Duong, L., Yang, D., Yunfel, X.F., Kloprogge, J.T., 2006. Changes in the morphology of organoclays with HDTMA(+) surfactant loading. Appl. Clay Sci. 31 (3–4), 262–271.

Ho, Y.S., McKay, G., 1998. Sorption of dye from aqueous solution by peat. Chem. Eng. J. 70 (2), 115–124.

Jarraya, I., Fourmentin, S., Benzina, M., Bouaziz, S., 2010. VOC adsorption on raw and modified clay materials. Chem. Geol. 275 (1–2), 1–8.

Jiang, J.Q., Cooper, C., Ouki, S., 2002. Comparison of modified montmorillonite adsorbents —part I: preparation, characterization and phenol adsorption. Chemosphere 47 (7), 711–716.

Juang, R.S., Lin, S.H., Tsao, K.H., 2002. Mechanism of sorption of phenols from aqueous solutions onto surfactant-modified montmorillonite. J. Colloid Interface Sci. 254 (2), 234–241.

Kasama, T., Watanabe, Y., Yamada, H., Murakami, T., 2004. Sorption of phosphates on Al-pillared smectites and mica at acidic to neutral pH. Appl. Clay Sci. 25 (3–4), 167–177.

Kim, Y.H., Kim, C.M., Choi, I.H., Rengaraj, S., Yi, J.H., 2004. Arsenic removal using mesoporous alumina prepared via a templating method. Environ. Sci. Technol. 38 (3), 924–931.

Kloprogge, J.T., 1998. Synthesis of smectites and porous pillared clay catalysts: a review. J. Porous. Mater. 5 (1), 5–41.

Lagaly, G., 1986. Interaction of alkylamines with different types of layered compounds. Solid State Ionics 22 (1), 43–51.

Moreno, S., Kou, R.S., Poncelet, G., 1997. Influence of preparation variables on the structural, textural, and catalytic properties of Al-pillared smectites. J. Phys. Chem. B 101 (9), 1569–1578.

Na, P., Jia, X.M., Bin, Y., Li, Y., Na, J., Chen, Y.C., Wang, L.S., 2010. Arsenic adsorption on Ti-pillared montmorillonite. J. Chem. Technol. Biotechnol. 85 (5), 708–714.

Ozcan, A., Omeroglu, C., Erdogan, Y., Ozcan, A.S., 2007. Modification of bentonite with a cationic surfactant: an adsorption study of textile dye Reactive Blue 19. J. Hazard. Mater. 140 (1–2), 173–179.

Park, S.J., Kim, Y.B., Yeo, S.D., 2008. Vapor adsorption of volatile organic compounds using organically modified clay. Sep. Sci. Technol. 43 (5), 1174–1190.

Peng, X.J., Luan, Z.K., Zhang, H.M., Tian, B.H., 2005. Zirconia pillared montmorillonite for removal of arsenate from water. J. Environ. Sci. Health A Tox. Hazard. Subst. Environ. Eng. 40 (5), 1055–1067.

Qin, Z., Yuan, P., Zhu, J., He, H., Liu, D., Yang, S., 2010. Influences of thermal pretreatment temperature and solvent on the organosilane modification of Al_{13}-intercalated/Al-pillared montmorillonite. Appl. Clay Sci. 50 (4), 546–553.

Salerno, P., Mendioroz, S., 2002. Preparation of Al-pillared montmorillonite from concentrated dispersions. Appl. Clay Sci. 22 (3), 115–123.

Shanmugharaj, A.M., Rhee, K.Y., Ryu, S.H., 2006. Influence of dispersing medium on grafting of aminopropyltriethoxysilane in swelling clay materials. J. Colloid Interface Sci. 298 (2), 854–859.

Shen, W., He, H.P., Zhu, J.X., Yuan, P., Frost, R.L., 2007. Grafting of montmorillonite with different functional silanes via two different reaction systems. J. Colloid Interface Sci. 313 (1), 268–273.

Sing, K.S.W., Everett, D.H., Haul, R.A.W., Moscou, L., Pierotti, R.A., Rouquerol, J., Siemieniewska, T., 1985. Reporting physisorption data for gas solid systems with special reference to the determination of surface-area and porosity (Recommendations 1984). Pure Appl. Chem. 57 (4), 603–619.

Sivaiah, M.V., Petit, S., Brendle, J., Patrier, P., 2010. Rapid synthesis of aluminium polycations by microwave assisted hydrolysis of aluminium via decomposition of urea and preparation of Al-pillared montmorillonite. Appl. Clay Sci. 48 (1–2), 138–145.

Tian, S.L., Zhu, L.Z., Shi, Y., 2004. Characterization of sorption mechanisms of VOCs with organobentonites using a LSER approach. Environ. Sci. Technol. 38 (2), 489–495.

Vadivelan, V., Kumar, K.V., 2005. Equilibrium, kinetics, mechanism, and process design for the sorption of methylene blue onto rice husk. J. Colloid Interface Sci. 286 (1), 90–100.

Valverde, J.L., Sanchez, P., Dorado, F., Asencio, I., Romero, A., 2003. Preparation and characterization of Ti-pillared clays using Ti alkoxides. Influence of the synthesis parameters. Clay Clay Miner. 51 (1), 41–51.

Valverde, J.L., Romero, A., Romero, R., Garcia, P.B., Sanchez, M.L., Asencio, I., 2005. Preparation and characterization of Fe-PILCs. Influence of the synthesis parameters. Clay Clay Miner. 53 (6), 613–621.

Vicente, M.A., Banares-Munoz, M.A., Toranzo, R., Gandia, L.M., Gil, A., 2001. Influence of the Ti precursor on the properties of Ti-pillared smectites. Clay Miner. 36 (1), 125–138.

Wang, S.B., Boyjoo, Y., Choueib, A., Zhu, Z.H., 2005. Removal of dyes from aqueous solution using fly ash and red mud. Water Res. 39 (1), 129–138.

Xi, Y.F., Frost, R.L., He, H.P., 2007. Modification of the surfaces of Wyoming montmorillonite by the cationic surfactants alkyl trimethyl, dialkyl dimethyl, and trialkyl methyl ammonium bromides. J. Colloid Interface Sci. 305 (1), 150–158.

Yuan, P., He, H.P., Bergaya, F., Wu, D.Q., Zhou, Q., Zhu, J.X., 2006a. Synthesis and characterization of delaminated iron-pillared clay with meso-microporous structure. Microporous Mesoporous Mater. 88 (1–3), 8–15.

Yuan, P., Yin, X.L., He, H.P., Yang, D., Wang, L.J., Zhu, J.X., 2006b. Investigation, on the delaminated-pillared structure of TiO_2-PILC synthesized by $TiCl_4$ hydrolysis method. Microporous Mesoporous Mater. 93 (1–3), 240–247.

Yuan, P., Annabi-Bergaya, F., Tao, Q., Fan, M.D., Liu, Z.W., Zhu, J.X., He, H.P., Chen, T.H., 2008a. A combined study by XRD, MR, TG and HRTEM on the structure of delaminated Fe-intercalated/pillared clay. J. Colloid Interface Sci. 324 (1–2), 142–149.

Yuan, P., Southon, P.D., Liu, Z.W., Green, M.E.R., Hook, J.M., Antill, S.J., Kepert, C.J., 2008b. Functionalization of halloysite clay nanotubes by grafting with gamma-aminopropyltriethoxysilane. J. Phys. Chem. C 112 (40), 15742–15751.

Zhou, Q., He, H.P., Zhu, J.X., Shen, W., Frost, R.L., Yuan, P., 2008. Mechanism of p-nitrophenol adsorption from aqueous solution by HDTMA+-pillared montmorillonite—implications for water purification. J. Hazard. Mater. 154 (1–3), 1025–1032.

Zhu, L.Z., Zhu, R.L., 2007. Simultaneous sorption of organic compounds and phosphate to inorganic–organic bentonites from water. Sep. Purif. Technol. 54 (1), 71–76.